

Comparison of Voltage-activated Cl⁻ Channels in Rat Parotid Acinar Cells with CIC-2 in a Mammalian Expression System

K. Park¹, J. Arreola^{1,2}, T. Begegnich², J.E. Melvin¹

¹Rochester Institute for Biomedical Sciences, Center for Oral Biology, University of Rochester Medical Center, Rochester, NY 14642, USA

²Department of Pharmacology and Physiology, University of Rochester Medical Center, Rochester, NY 14642, USA

Received: 10 November 1997/Revised: 19 February 1998

Abstract. Rat parotid acinar cells express Cl⁻ currents that are activated in a time-dependent manner by hyperpolarized potentials. CIC-2, a member of the CIC gene family, codes for a voltage-gated, inward rectifying anion channel when expressed in *Xenopus* oocytes. In the present study, we found that cDNA derived from individual parotid acinar cells contained sequence identical to that reported for CIC-2 in rat brain and heart. A polyclonal antibody generated against the N-terminal cytoplasmic domain of CIC-2 recognized an approximately 100 kD protein on western blots of both brain and parotid gland. CIC-2 expressed in oocytes has different kinetics from the currents found in parotid acinar cells. Since the CIC-2 channel was cloned from and its transcripts are expressed in mammalian tissue, we compared the channel properties of acinar cells to a mammalian expression system. We expressed CIC-2 channels in human embryonic kidney cells, HEK 293, using recombinant CIC-2 DNA and CIC-2 DNA fused with DNA coding for jellyfish green fluorescent protein (GFP). Confocal microscopy revealed that the expressed CIC-2-GFP chimera protein localized to the plasma membrane. Whole cell Cl⁻ currents from HEK 293 cells expressing CIC-2-GFP were similar, if not identical, to the Cl⁻ currents recorded from cells transfected with CIC-2 cDNA (no GFP). The voltage-dependence and kinetics of CIC-2 channels expressed in HEK 293 cells were quite similar to those in acinar cells. Channels in parotid acinar and HEK 293 cells activated at more positive membrane potentials and with a faster time course than the channels expressed in *Xenopus* oocytes. In summary, we found that CIC-2 message and protein are expressed in salivary cells and that the properties of voltage-activated, inward

rectifying Cl⁻ channels in acinar cells are similar to those generated by the CIC-2-GFP construct expressed in HEK 293 cells. The properties of the CIC-2 anion channel seem to be dependent on the type of cell background in which it is expressed.

Key words: Salivary acinar cells — HEK 293 — Green fluorescent protein

Introduction

The CIC gene family codes for several types of voltage-gated chloride channel proteins (Jentsch et al., 1995; Jentsch, 1996; Jentsch & Günther, 1997). One member of this family, CIC-2, was first cloned from rat brain and heart and its transcripts are widely expressed in mammalian tissues and cell lines (Thiemann et al., 1992). The functional properties of this channel have been characterized by transient expression in *Xenopus* oocytes (Thiemann et al., 1992; Gründer et al., 1992; Jordt & Jentsch, 1997). When expressed in oocytes, CIC-2 is activated by hyperpolarization and cell swelling. Hyperpolarization-activated chloride currents have been identified in several cell types such as neurons (Smith et al., 1995), pancreatic acinar cells (Carew & Thorn, 1996), mandibular gland duct cells (Dinudom, Young & Cook, 1993; Komwatana et al., 1994), Leydig cells from mature testis (Noulin & Joffre, 1993), intestinal T84 cells (Fritsch & Edelman, 1996), osteoblasts (Chesnoy-Marchais & Fritsch, 1994), and parotid acinar cells (Arreola et al., 1996).

The properties of these Cl⁻ currents are generally similar to the CIC-2 Cl⁻ channels expressed in oocytes. However, several distinct differences are evident, e.g., in anion selectivity and inhibitor sensitivity, making it difficult to positively identify endogenous voltage-activated

Cl⁻ currents as CIC-2. In parotid acinar cells the hyperpolarization-activated channels are equally permeable to Cl⁻ and I⁻ (Arreola et al., 1996). When expressed in oocytes, rat CIC-2 displays strong selectivity for Cl⁻ over I⁻ (Thiemann et al., 1992) whereas rabbit CIC-2 favors I⁻ over Cl⁻ (Malinowska et al., 1995). CIC-2 is apparently activated by hypotonic shock and is sensitive to the Cl⁻ channel blockers DPC and 9-AC (Thiemann et al., 1992; Gründer et al., 1992; Jordt & Jentsch, 1997), while the CIC-2-like currents in mouse mandibular gland duct cells (Komwatana et al., 1995) and rat osteoblasts (Chesnoy-Marchais & Fritsch, 1994) are inhibited by cell swelling and are insensitive to these same antagonists. The voltage-activated Cl⁻ current in rat osteoblastic cells is much more sensitive (Chesnoy-Marchais & Fritsch, 1994) to DIDS inhibition than CIC-2 channels expressed in oocytes (Thiemann et al., 1992). It is unclear whether the different properties of the Cl⁻ currents in oocytes expressing CIC-2 are the result of altered characteristics of these Cl⁻ currents when expressed in a non-mammalian background or that the hyperpolarization-activated Cl⁻ currents in mammalian cells are not due to the CIC-2 protein.

The transient expression of cloned ion channels in *Xenopus* oocytes is a common method to study channel properties. However, Cl⁻ channel expression in these oocytes is complicated by the presence of endogenous chloride channels (Kowdley et al., 1994). On the other hand, the identification of transfected cells is difficult in mammalian transient expression systems. One strategy for easily identifying transfected cells is labeling channels with the green fluorescent protein (GFP) as has been successfully used to study the functional expression of NMDAR1 receptor-activated anion channels (Marshall et al., 1995). GFP, cloned from the jellyfish *Aequorea victoria*, is a cytosolic polypeptide composed of 238 amino acid residues which emits green fluorescent light in the absence of exogenous substrates and cofactors when expressed in *E. coli* or mammalian cells (Prasher et al., 1992). It has been shown to be an excellent tool for following protein expression, localization, and trafficking without any noticeable functional disruption of the protein being studied (Chalfie et al., 1994; Marshall et al., 1995).

The purpose of the present study was to compare the kinetic properties of native voltage-activated Cl⁻ currents with CIC-2 expressed in a well-defined mammalian expression system. In this communication we demonstrate that CIC-2 transcript and protein are expressed in rat parotid glands. We also describe the properties of a chimera CIC-2 chloride channel fused to the GFP reporter gene. The chimera CIC-2-GFP channels produced a fluorescent protein localized to the plasma membrane when expressed in the human embryonic kidney cell line HEK 293. The electrophysiological properties of the

CIC-2-GFP channel activated by hyperpolarizing membrane potentials were similar to those of parotid acinar cells. In contrast, the voltage sensitivity and activation kinetics of the CIC-2 channels from these mammalian cells were quite different than those of the CIC-2 channel expressed in *Xenopus* oocytes.

Materials and Methods

PREPARATION OF RAT PAROTID ACINAR CELLS

Parotid glands were removed from male 150–250 gm Wistar strain rats and dispersed by trypsin-collagenase digestion as described previously (Arreola et al., 1996). Acinar cells were plated onto poly-L-lysine coated glass coverslips for patch clamp experiments. Individual acinar cells were collected using glass micropipettes for RT-PCR experiments.

RT-PCR AMPLIFICATION OF RAT PAROTID ACINAR CELLS

Total RNA was isolated from 5–10 acinar cells using either the Hirt supernatant method (1967) or TRIzol reagent (Gibco BRL, Grand Island, NY). RNA was reverse-transcribed to cDNA according to the manufacturer's instructions (1st-STRAND cDNA Synthesis kit, Clontech, Palo Alto, CA). The cDNA was amplified using PCR primer sets that covered the entire protein coding region of the rat CIC-2 gene. The 50 µl PCR reaction mixture contained 5 µl of the cDNA-containing solution, 0.2 µM of the upper and lower primers, 3 µl of 25 mM MgCl₂, 4 µl of 2.5 mM dNTPs, 5 µl of 10× PCR buffer (500 mM KCl, 100 mM Tris-HCl, pH 8.3) and 0.4 µl (2 U) of AmpliTaq DNA polymerase (Perkin-Elmer, Norwalk, CT). PCR amplification was carried out for 30 cycles in a DNA thermal cycler (MJ Research, Watertown, MA) and each cycle was set to: 94°C for 30 sec, 68°C for 20 sec, 72°C for 2 min. A 2-µl aliquot of the first-round PCR reaction mixture was re-amplified using the same PCR conditions. PCR amplification products were separated on 1% TBE-agarose gels and further analyzed by restriction endonucleases and by Sanger DNA sequencing (Sanger, Nicklen & Coulson, 1977).

Based on published sequence (Thiemann et al., 1992), rat CIC-2 specific primers were synthesized as follows:

1. **CIC2U1**, 5'(-33)AAGCAAGAGGAGGCAAGAGGAC(-12)-3'
2. **CIC2U2**, 5'-(309)GGGGCTCCTCATGGCATTGGTCAGT(333)-3'
3. **CIC2U3**, 5'-(885)TCGGGTCTTGGCAGTGTGGAACCGTGA-T(912)-3'
4. **CIC2U4**, 5'-(2036)TCCGCTTCCAGGTGAACACAGAGGAC-T(2062)-3'
5. **CIC2L1**, 5'-(1025)GCTCCCCGAAGCCACTAGCAATAC-(1001)-3'
6. **CIC2L2**, 5'-(2127)GGGCCCTCTCTTTAGAGCAGGCTTCA-G(2101)-3'
7. **CIC2L3**, 5'-(2902)TTCTCAAAGACGAGGCAGGGG(2881)-3'

the numbers in parentheses refer to the nucleotide positions in the CIC-2 gene assigning the value +1 to the translation initiation site.

CLONING OF THE CODING REGION FOR THE CIC-2 GENE FROM RAT BRAIN

Poly(A⁺) RNA was prepared from rat brain by oligo(dT)-cellulose chromatography of total RNA isolated by TRIzol reagent. First strand

cDNA was reverse-transcribed from Poly(A⁺) RNA as above. Oligonucleotide primers CIC2U1 and CIC2L3 were used to amplify a 2935 bp product containing the entire protein coding sequence for CIC-2. PCR amplifications were carried out for 30 cycles under the above PCR conditions. The amplified CIC-2 cDNA was gel purified and subcloned into the pCRII vector (Invitrogen, San Diego, CA) for further analyses. The CIC-2 DNA sequence was confirmed by sequencing.

CONSTRUCTION OF CIC-2 cDNA IN pcDNA1

EcoRI endonuclease (New England Biolabs, Beverly, MA) was used to digest CIC-2 cDNA from pCRII-CIC-2. CIC-2 expression was driven by the cytomegalovirus mammalian promoter after insertion into the pcDNA1 vector (Invitrogen, San Diego, CA), pcDNA1-CIC-2. The correct orientation for translation of the DNA was confirmed by sequencing.

SITE-DIRECTED MUTAGENESIS AND CONSTRUCTION OF CIC-2-GFP cDNA IN THE pMT3 VECTOR

CIC-2 cDNA was mutated using a PCR-based technique (Saiki et al., 1988) to introduce an AgeI restriction endonuclease site and to remove the 3' end stop codon. The synthesized lower primer to produce these mutations had the following sequence:

5'-(2726)GGTCACcGGtaACTTGTCa(2709)-3'

This lower primer and the CIC2U1 upper primer (*see above*) were employed to amplify and mutate pCRII-CIC-2 cDNA. The lower case letters in the mutating primer sequence indicate the base changes. The PCR products were digested by AgeI and gel purified. The purified fragment was subcloned into the pMT3-GFP vector which had been linearized by AgeI and dephosphorylated with calf intestine alkaline phosphatase (Boehringer Mannheim Biochemica, Germany). The pMT3-GFP plasmid contains GFP cDNA inserted in the KpnI and SpeI sites of the pMT3 vector. The pMT3 vector was derived from pMT2 by replacing the multi-cloning sites for the PstI and EcoRI cloning sites (Franke et al., 1988). After ligation of the AgeI sticky-ends of the pMT3-GFP vector and the mutated CIC-2 cDNA, the free ends were blunt-ended using T4 DNA polymerase (New England Biolabs, Beverly, MA) and self-ligated. The pMT3-CIC-2-GFP fusion construct was sequenced to confirm the mutation and orientation.

TRANSIENT EXPRESSION OF GFP, CLC-2-GFP, AND CIC-2 PROTEINS IN HEK 293 CELLS

The human embryonic cell line HEK 293 (American Type Culture Collection, Rockville, MD) was maintained in Dulbecco's modified Eagle's medium containing 10% newborn calf serum, 2 mM L-glutamine, penicillin (100 units ml⁻¹) and streptomycin (100 µg ml⁻¹; Gibco/BRL, Grand Island, NY). One day prior to transfection, cells were replated (5 × 10⁵ cells per 60 mm plate) and then transfected with 10 µg of plasmid DNA (pcDNA1-CIC-2, pMT3-CIC-2-GFP, or pMT3-GFP plasmid DNA) using the calcium precipitation method (Chen & Okayama, 1987). Fifty µl of 2.5 M CaCl₂ was added to 450 µl of plasmid DNA (10 µg) in 0.1× TE (1 mM Tris-HCl, 0.1 mM EDTA, pH = 8.0). This mixture was added to 500 µl of 2× HEPES-buffered saline (280 mM NaCl, 50 mM HEPES, 1.5 mM Na₂HPO₄, pH = 7.1) and precipitated for 30 min at room temperature. The cells were incubated with the Ca²⁺ phosphate-DNA precipitates for 6 hr, followed by a 10% glycerol shock for 3 min and then incubated with fresh medium.

RECOVERY OF pcDNA-1-CIC-2 FROM HEK 293 CELLS

Plasmid DNA from HEK 293 cells was rescued using the Hirt extraction method (1967) to verify that the recorded inward rectifying Cl⁻ currents were due to expression of CIC-2 cDNA lacking the GFP label. The cells were collected with a glass micropipette and lysed in 0.8 ml of 0.6% SDS containing 0.01 M EDTA (pH = 7.5) for 20 min at room temperature. Two hundred µl of 5 M NaCl was added to the lysate, mixed gently by inverting the tube 10 times, and stored at 4°C for at least 8 hr. After centrifugation at 17,000 × g for 30 min at 4°C, the supernatant was removed and precipitated with 100% ethanol. The recovered plasmid DNA was transformed into the *E. coli* strain JM109 using electroporation (1 × 10⁹ cfu per µg plasmid DNA) and analyzed by restriction endonuclease digestion with KpnI.

IDENTIFICATION OF EXPRESSED AND NATIVE CIC-2 USING WESTERN BLOT ANALYSIS

A rabbit polyclonal antibody was prepared to the N-terminal region of rat CIC-2 corresponding to amino acids Met 16 to Glu 35 (oligopeptide MEPRALQYEQTLMYGRYTQE). The anti-CIC-2 antibody was purified using an antigen (the synthesized oligopeptide)-linked affinity column.

Rat brain homogenates and rat parotid crude membranes were used to identify native CIC-2 protein. Tissues were prepared as previously described by Turner, George & Baum (1986). Rat brains and parotid glands were homogenized twice by 10-sec strokes at power level 5 with a Polytron homogenizer (Brinkmann Instruments, Westbury, NY) in 10 ml per gram tissue of a solution containing: 10 mM HEPES adjusted to pH 7.4 with Tris, 10% sucrose, 1 mM EDTA and 1 mM PMSF. Homogenates were centrifuged at 2,500 × g for 15 min at 4°C and the supernatants were saved. Rat parotid glands were further purified to prepare crude membrane proteins by centrifugation of the supernatant at 22,000 × g for 20 min at 4°C. The supernatant was discarded and the pellet was resuspended in buffer (10 mM HEPES adjusted to pH 7.4 with Tris, 100 mM mannitol, 1 mM EDTA and 1 mM PMSF), passed once through a 25-gauge needle and once through a 30-gauge needle. Aliquots were quickly frozen in liquid N₂ and stored at -85°C until use.

Cell extracts from transfected HEK 293 cells were used to identify expressed CIC-2 protein. Extracts were prepared 48 hr after transfection. HEK 293 cells were washed twice with PBS and centrifuged at 700 × g for 10 min. Proteins were extracted in 10% SDS with boiling for 5 min followed by addition of an equal volume of lysis buffer (250 mM sucrose, 5 mM MOPS, 1 mM EDTA, pH = 7.5, and 1 mM PMSF) and stored at -85°C until use.

Protein concentration was determined using the BCA (bicinchonic acid) protein assay reagent (Pierce, Rockford, IL). Proteins (70 µg/lane) were resolved by 10% SDS-PAGE and transferred to a nitrocellulose membrane (hybond C, Amersham, Arlington Heights, IL). Membranes were blocked in PBS containing 0.1% tween 20, 10% normal goat serum and 4% BSA and probed with the affinity column purified primary antibody (anti-CIC-2) or pre-immune serum. Proteins were then detected with a horseradish peroxidase-conjugated goat anti-rabbit IgG antibody (Jackson ImmunoResearch Lab., West Grove, PA) by ECL chemiluminescence (Amersham, Buckinghamshire, England).

IDENTIFICATION OF EXPRESSED GFP OR CIC-2-GFP IN HEK 293 CELLS BY CONFOCAL MICROSCOPY

The fluorescence from cells expressing either the CIC-2-GFP fusion or GFP gene product was viewed on an Ultima confocal laser cytometer (Meridian Instr., Okemos, MI) using an Olympus 40× UV objective

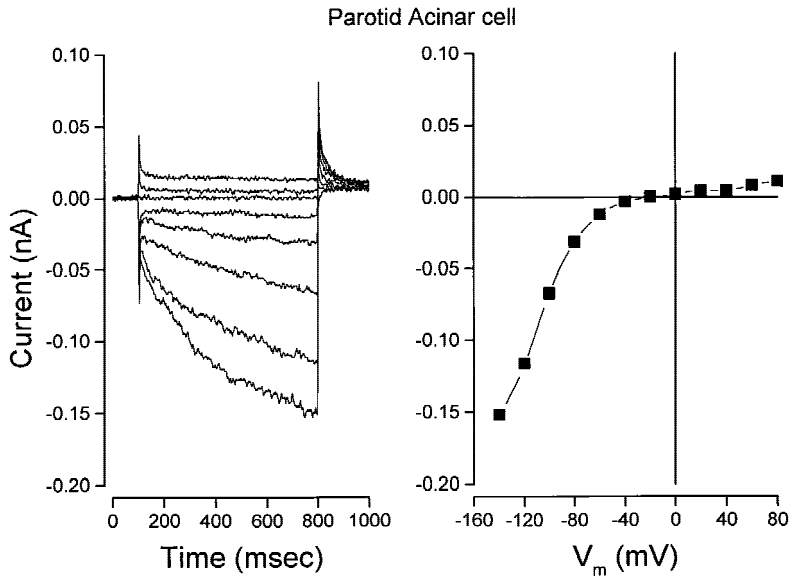


Fig. 1. Voltage-activated current in rat parotid acinar cells. *Left panel:* Whole-cell currents in response to 700 msec voltage pulses to +80, +40, 0, -60, -80, -100, -120, and -140 mV from a holding potential of 0 mV. *Right panel:* Currents measured at the end of the pulses in the left panel at the indicated voltages.

(NA 0.85). GFP was excited with the 488 nm wavelength of an Enterprise argon laser (Coherent, CA) and the emitted fluorescence was monitored at >500 nm. The estimated thickness of the image was 5 μ m. Forty-eight hours after transfection, the Cl^- currents of fluorescent cells were recorded with the whole-cell patch clamp technique.

WHOLE-CELL PATCH CLAMP

The whole cell configuration of the patch clamp technique was used to record macroscopic Cl^- currents from rat parotid acinar cells and from HEK 293 cells 48 hr after transfection. Cl^- currents were recorded with a PC-501A amplifier (Warner Instrument). Pipettes had 1–2 M Ω resistance when filled with the internal solution. Cation currents were minimized using the non-permeant cation TEA inside and outside the cell. To facilitate comparison with previous observations of voltage-activated Cl^- channels in native parotid acinar cells (Arreola et al., 1996) we used the same intracellular solution which was composed of (in mM): 135 TEACl, 5 TEAF, 15 EGTA-TEA, and 20 TES pH 7.3. Cells were bathed in a pH 7.3 hypertonic solution containing (in mM): 135 TEACl, 15 EGTA-TEA, 20 TES, and 60 D-mannitol. This hypertonic bath solution inactivates the endogenous volume-sensitive Cl^- current present in parotid acinar cells and HEK 293 cells.

Whole cell current recordings began 5–8 min after rupturing the plasma membrane beneath the pipette tip except for experiments designed to monitor the time dependent increase in the magnitude of the voltage-gated, inward rectifying Cl^- currents. The holding potential was 0 mV. To activate CIC-2 channels the membrane potential was stepped every 10 sec to values from -140 to +80 mV in 20 mV increments of 500–700 msec duration each. In most experiments the voltage was repolarized to -50 mV for an additional 300–500 msec before returning to the holding potential. Capacitative transients were partly compensated by the amplifier circuitry. Macroscopic currents were filtered at 500 Hz and sampled at 250 or 667 Hz.

Results

VOLTAGE-GATED, INWARD RECTIFYING Cl^- CURRENTS IN RAT PAROTID ACINAR CELLS

Rat parotid acinar cells express at least three types of anion channels (Arreola et al., 1996). One of these ex-

presses slowly activating, voltage-dependent currents as illustrated in Fig. 1. The left panel contains time-dependent currents activated by voltage-clamp pulses to potentials between +80 and -140 mV (top to bottom). Steps to positive potentials produced rather little current but steps to negative potentials evoked larger, time dependent currents. The right panel shows the voltage-dependence of the current measured at the end of the voltage clamp steps.

The substantial inward rectification seen in the data in right panel of Fig. 1 is generally similar to the properties of CIC-2 channels expressed in *Xenopus* oocytes (Thiemann et al., 1992). However, the current kinetics (Fig. 1, left panel) are considerably faster than CIC-2 currents expressed in oocytes. Nevertheless, the generally similar properties of CIC-2 in oocytes and the currents in rat parotid acinar cells, combined with evidence for CIC-2 transcripts in whole gland tissue (Arreola et al., 1996), raises the possibility that the observed acinar currents arise from CIC-2 proteins. The first requirement for such an identification is the expression of CIC-2 in acinar cells, not just in whole gland tissue.

CIC-2 EXPRESSION IN SINGLE RAT PAROTID ACINAR CELLS

Acinar cells comprise about 80% of the rat parotid gland and therefore leaves open the possibility that the signal detected in this previous study was due to CIC-2 transcripts present in non-acinar cells (Arreola et al., 1996). Therefore, individual acinar cells were isolated by micropipette and analyzed for CIC-2 transcripts. Rat CIC-2 specific primers were designed to amplify the entire protein coding region. Sequence analysis of the cDNA products from RT-PCR verified that transcripts identical

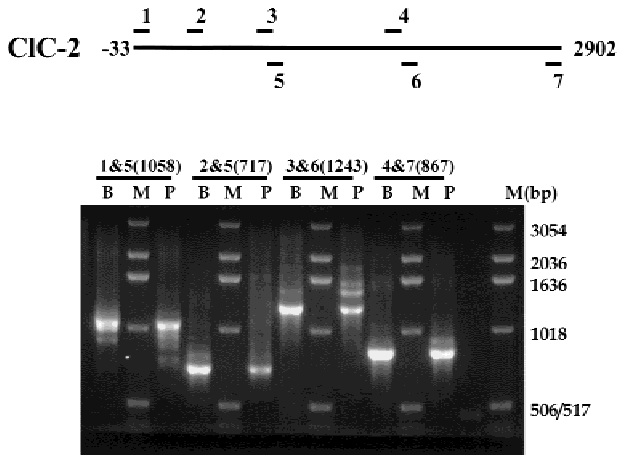


Fig. 2. RT-PCR of CIC-2 transcripts in rat parotid acinar cells. Individual acinar cells and acini were isolated by micropipette. The position of the upper and lower rat CIC-2 specific primers used to amplify the entire protein coding region are shown in the upper panel. In the lower panel, the primer pairs used and the expected size products (given in parentheses) are shown above the amplified products from brain (B) and parotid acinar cells (P). Molecular weight markers (M) are shown (1 Kb ladder, GibcoBRL). The image was digitized with an IS-1000 imaging system (Alpha Innotech, San Leandro, CA). Sequence analysis of the products from RT-PCR of RNA isolated from these cells verified that transcripts identical to rat brain CIC-2 were present in rat parotid acinar cells.

to rat brain CIC-2 were present in rat parotid acinar cells (Fig. 2).

An affinity-purified polyclonal antibody was used to confirm that CIC-2 protein was expressed in rat parotid gland. Panel B of Fig. 3 shows the results testing the specificity of the antibody generated against the N-terminal domain of CIC-2. Proteins isolated from HEK 293 cells (Lane 1) showed no reactivity with the antibody, whereas the antibody recognized a distinct band in protein extracts from HEK 293 cells transfected with both a CIC-2 containing plasmid (Lane 2) and a CIC-2-GFP containing plasmid (Lane 3). CIC-2-GFP migrated with a molecular weight of about 125 kD, the expected size of the fusion protein, whereas CIC-2 expressed in HEK 293 cells migrated somewhat faster than anticipated with a molecular weight of 85–90 kD. Panel A of Fig. 3 shows that pre-immune serum (PI) did not react with proteins isolated from rat parotid gland (P) or brain (B), the tissue from which CIC-2 was cloned. In contrast, the affinity-purified antibody (Ab) recognized a protein band in both parotid gland and brain of about 100 kD, the size protein predicted from the CIC-2 cDNA sequence analysis. Additional smaller molecular weight bands are also present in brain tissue homogenates. Modifying the protease inhibitor cocktail did not change the relative abundance of the various protein bands in brain homogenates suggesting that proteolysis during the protein isolation procedure was not responsible for the

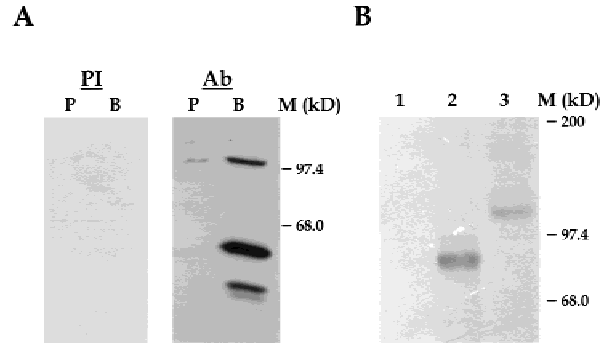


Fig. 3. Western analysis of CIC-2 protein in rat parotid gland and brain. An affinity-purified polyclonal antibody was used to confirm that CIC-2 protein is present in rat parotid gland. *Panel A:* pre-immune serum (PI) did not react with proteins isolated from rat parotid gland (P) or brain (B). The affinity-purified antibody (Ab) recognized a protein band in both parotid gland and brain of about 100 kD, the size protein predicted from CIC-2 cDNA sequence analysis. *Panel B:* Proteins isolated from HEK 293 cells (Lane 1) showed no reactivity with the antibody, whereas the antibody recognized distinct bands in protein extracts from HEK 293 cells transfected with both a CIC-2 containing plasmid (Lane 2) and a CIC-2-GFP containing plasmid (Lane 3). The image was digitized with an IS-1000 imaging system (Alpha Innotech, San Leandro, CA).

multiple bands on the Western blot. These smaller molecular weight bands may represent some post-translation event or cross-reactivity with a related protein in brain tissue.

The data of Figs. 2 and 3 demonstrate that CIC-2 was expressed in rat parotid acinar cells—a necessary requirement to identifying the inwardly rectifying current with this channel protein. However, the differences in kinetics between CIC-2 expressed in oocytes and the kinetics of the inwardly rectifying current in acinar cells make this identification less certain. To examine if the CIC-2 kinetics depended on the expression system used, we studied CIC-2 properties as expressed in mammalian HEK 293 cells.

IDENTIFICATION OF TRANSFECTED CELLS BY GFP FLUORESCENCE

The identification of transfected cells was facilitated by fusing GFP cDNA to the carboxyl terminus of CIC-2 cDNA. The carboxyl terminus was chosen because mutation analysis of CIC-2 expressed in *Xenopus* oocytes showed that this domain is not involved in channel gating, whereas the amino terminus is necessary for channel activation by volume and voltage (Gründer et al., 1992; Jordt & Jentsch, 1997). GFP fluorescence was viewed by confocal microscopy 48 hr after transfection. Cells transfected with GFP cDNA produced a homogenous fluorescence throughout the cytosol (Fig. 4, upper panel). In contrast, the expressed chimera CIC-2-GFP produced

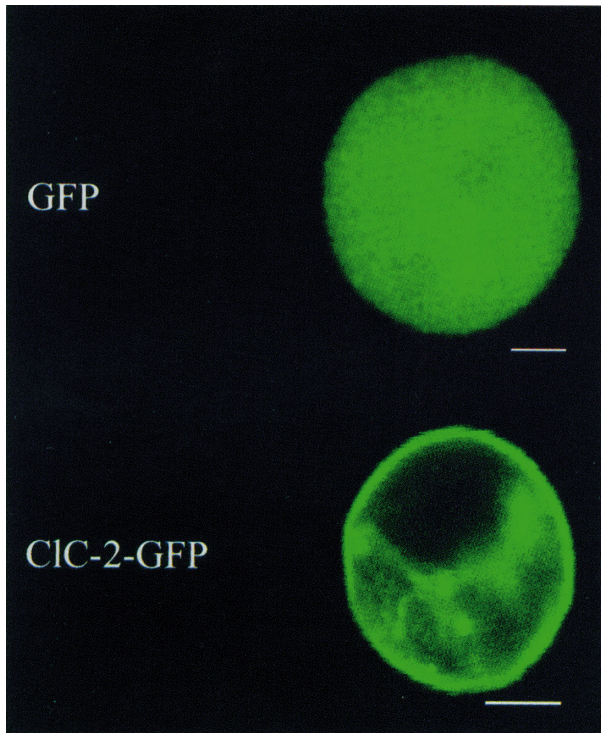


Fig. 4. Confocal imaging of GFP and CIC-2-GFP proteins in HEK 293 cells. The GFP fluorescence emitted from transfected cells were viewed by confocal microscopy. *Upper panel:* cell transfected with GFP. *Lower panel:* cell transfected with the CIC-2-GFP chimera protein. Scale bars indicate 5 μm , thickness of the section is estimated to be around 5 μm .

fluorescence primarily distributed to the plasma membrane (lower panel of Fig. 4). The distribution of GFP fluorescence indicates that the chimera CIC-2-GFP protein sorted to the cell surface.

WHOLE CELL RECORDINGS FROM HEK 293 CELLS

Very little current over the voltage range from -140 to $+80$ mV was recorded from HEK 293 cells transfected only with GFP cDNA (upper left panel of Fig. 5). The right panel of Fig. 5 shows the average current-voltage relation obtained from four cells transfected with GFP cDNA (\bullet). The average currents at -140 and $+80$ mV were -0.12 ± 0.01 and $+0.19 \pm 0.01$ nA, respectively. This level of current was comparable to that observed in non-transfected cells (*data not shown*) and thus represents the limits of the background current in HEK 293 cells.

In contrast, cells transfected with the CIC-2-GFP construct displayed large inward currents. The lower left panel of Fig. 5 shows current traces obtained from -140 to $+80$ mV from a transfected cell identified by its fluorescence. Time-dependent currents were activated at

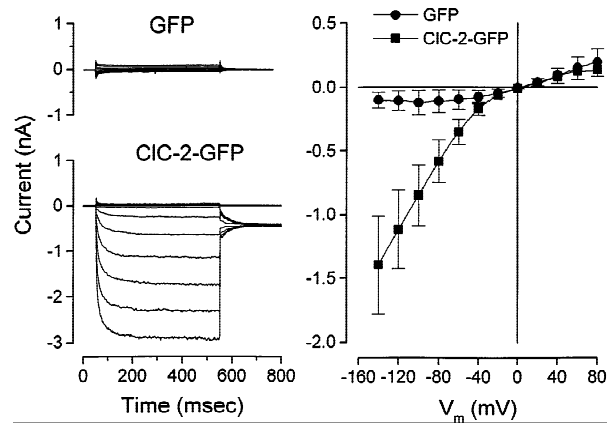


Fig. 5. Whole cell recordings from HEK 293 cells expressing either GFP or CIC-2-GFP protein. *Upper left panel:* Superimposed whole cell records from a HEK 293 cell transfected with GFP cDNA. Currents elicited by voltage steps to -140 to $+80$ mV in 20 mV increments from a 0 mV holding potential. *Lower left panel:* Superimposed whole cell records from a fluorescent HEK 293 cell transfected with CIC-2-GFP cDNA. Currents obtained by stepping the membrane potential from -140 to $+80$ mV in 20 mV increments from a 0 mV holding potential all followed by a step to -50 mV. *Right panel:* Mean current-voltage relation obtained from HEK 293 cells transfected with either GFP cDNA (\bullet , $n = 4$) or CIC-2-GFP cDNA (\blacksquare , $n = 6$). Currents were measured at the end of the test pulse.

negative potentials and approached a steady-state in 200–400 msec. The size of the currents decreased at more positive potentials. The current-voltage relation constructed from the amplitude of the current measured at the end of the test pulse is shown in the right panel of Fig. 5 (\blacksquare , $n = 6$). The CIC-2-GFP channel currents showed strong inward rectification. Indeed, the currents at potentials more positive than -20 mV were indistinguishable from the currents in GFP transfected cells at positive potentials suggesting that CIC-2 is not activated at positive potentials. The currents from the CIC-2-GFP channel were larger than background at potentials more negative than -20 mV.

We also examined currents in HEK 293 cells transfected with CIC-2 lacking the GFP tag. Most cells expressed very small currents, equivalent to those of cells transfected with GFP alone (Fig. 5, upper left panel). A very few cells expressed large, time dependent and inwardly rectifying currents as in the examples of Fig. 6. These cells were expressing CIC-2 as confirmed by restriction enzyme analysis of the rescued plasmid DNA (*data not shown*). We were unable to detect plasmid DNA in the cells that did not express large inwardly rectifying currents.

The results seen in Fig. 6 show that the GFP tag on CIC-2 had no large effect on the kinetics and voltage-dependence of the expressed current. The left panel contains currents recorded under conditions identical to those for the experiment of Fig. 5 and these appear quite

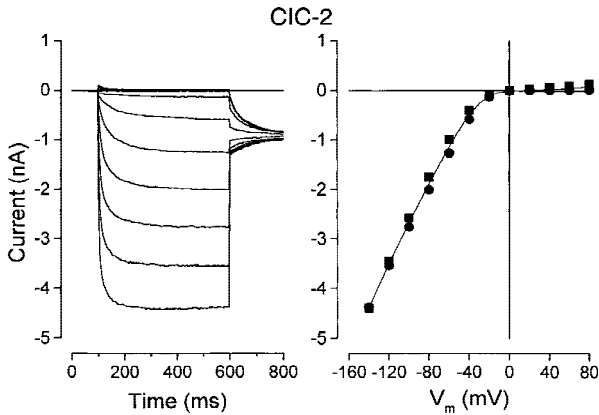


Fig. 6. Properties of CIC-2 chloride channels expressed in HEK-293 cells. *Left panel:* Superimposed macroscopic currents from a cell transfected with CIC-2 DNA. Currents obtained by stepping the membrane potential from -140 to $+80$ mV in 20 mV increments from a 0 mV holding potential all followed by a step to -50 mV. *Right panel:* Current-voltage relation for two different cells transfected with CIC-2 cDNA. Currents were measured at the end of the test pulse.

similar to the currents of CIC-2 with the GFP tag. The current-voltage relation of CIC-2 channels without the GFP tag (Fig. 6, right panel) is also quite similar to channels lacking GFP (Fig. 5, right panel).

The similarity between the rectification of CIC-2 channels is quantitatively addressed in Fig. 7. In this figure the currents have all been normalized to unity at -140 mV in order to allow comparison independent of the level of expression. The mean values of CIC-2-GFP from Fig. 5 are shown (●) and are quite similar to the CIC-2 data (○, □) from duplicate experiments without GFP. Also shown are data from rat parotid acinar cells (■) and these deviate only slightly from the CIC-2 results.

Figure 8 presents a quantitative analysis of the kinetics of CIC-2 channels expressed in HEK 293 cells. As shown in the inset, most of the time dependence of current activation could be described by a single exponential time function. There was a variable amount of the current (especially at more negative potentials) that could not be accounted for by a single exponential but, as seen in the inset, this component was rather small and quite slow. Consequently, we based our kinetic analysis on the dominant component clearly attributable to expression of CIC-2.

The main part of Fig. 8 shows the time constants from the exponential fits to the data at the potentials indicated. There appears to be rather little, systematic difference between the kinetics of CIC-2 channels (filled symbols) and those with the GFP tag (open symbols). The channel kinetics are seen to be accelerated at both very positive and very negative potentials.

All time constants in Fig. 8 at potentials more negative than -40 mV were obtained by voltage clamp steps

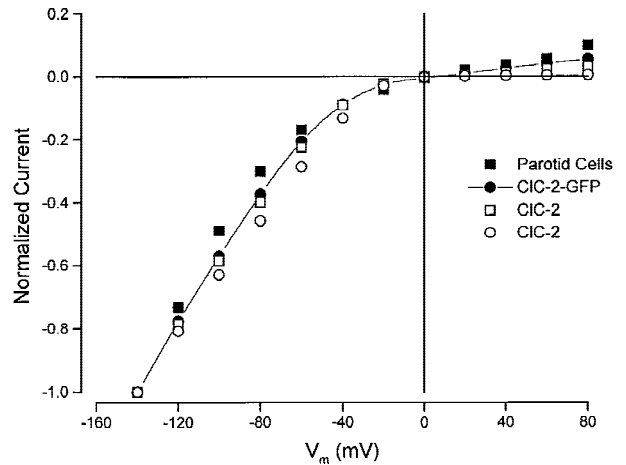


Fig. 7. Comparison of current voltage relations of CIC-2 channels and the inwardly rectifying current in parotid acinar cells. Whole-cell currents recorded from rat parotid acinar cells (■) and HEK 293 cells transfected with CIC-2 (○ □) and CIC-2-GFP (●) cDNA. All currents normalized to unity at -140 mV.

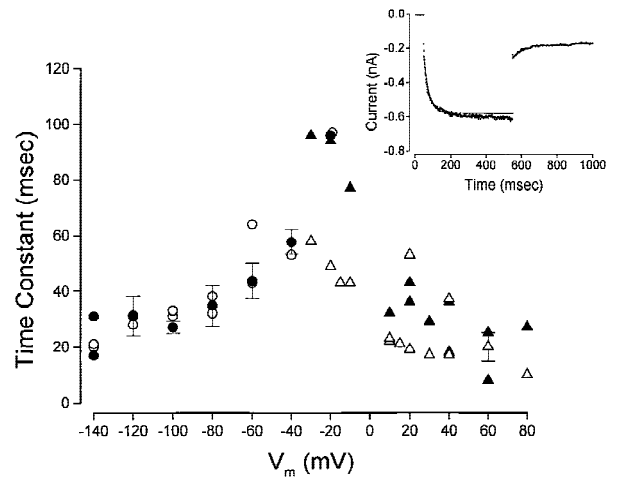


Fig. 8. Gating kinetics of the CIC-2 channels expressed in HEK 293 cells. Inset: Current (from a HEK 293 cell transfected with CIC-2-GFP) recorded during a pulse to -100 mV (points) superimposed with the fit of a single exponential time function (line) with a time constant of 28 msec. Figure: time constants from exponential fits to data at the indicated potentials. Activation data from cells transfected with CIC-2 (●) and CIC-2-GFP (○) cDNA and deactivation data from cells transfected with CIC-2 (▲) and CIC-2-GFP (△) cDNA. At potentials that include data from 3 or more cells the mean and SEM limits are shown. See text for additional details.

to these potentials from a positive holding potential at which the channels are mostly closed. These are activation time constants and denoted in the figure by circles. Most of the data in Fig. 8 at potentials positive to -40 mV were obtained by first activating the channels with a large negative voltage and determining the time constant of the current following repolarization to more positive

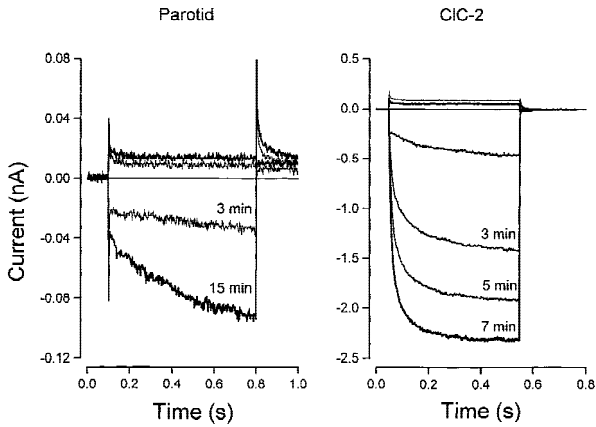


Fig. 9. Time-dependent increase in the voltage-activated current in rat parotid acinar cells and HEK 293 cells expressing CIC-2-GFP. Whole-cell currents at membrane potentials of -120 and $+60$ mV from a holding potential of 0 mV. *Left panel:* Currents from a rat parotid acinar cell collected at 3 (thin line) and 15 minutes (thick line) after obtaining the whole-cell mode. *Right panel:* Inward currents recorded at -120 mV from a HEK 293 cell expressing CIC-2-GFP recorded right after achieving whole cell mode and 3, 5, and 7 (thick line) minutes later (top to bottom). Outward current at $+60$ mV recorded at time 0 (thin line) and after 7 min (thick line).

potentials. This process represents channel closing or deactivation and the associated time constants are shown in Fig. 8 as triangles. In a few cases we were able to obtain both activation and deactivation near similar potentials (e.g., compare triangles and circles near -20 and $+20$ mV) and these appeared to be rather similar. This result suggests that CIC-2 channels as expressed in HEK 293 cells have a single open and a single closed state coupled by voltage dependent rate constants.

The expression of the inwardly rectifying currents in rat parotid acinar cells is not particularly robust (compare the acinar cell data of Fig. 1 with the CIC-2 currents in Figs. 5 and 6). We were, however, able to determine the time constants of acinar cell currents at very negative and at very positive potentials where there is a large driving force for Cl^- movement. These values were 750 ± 99 ($n = 5$), 1250 ± 180 ($n = 4$), and 450 ± 82 ($n = 3$) msec at -120 , -100 , and $+60$ mV, respectively. Thus, the channels in the native cell had kinetics more than an order of magnitude slower than CIC-2 expressed in HEK 293 cells.

Inwardly rectifying Cl^- channels have been observed in cells other than rat parotid acinar cells (Chesnoy-Marchais & Fritsch, 1994; Fritsch & Edelman, 1996). One property commonly noted in these other preparations is the slow increase in the magnitude of these currents with a concomitant increase in activation kinetics. The left panel of Fig. 9 shows that the Cl^- current in parotid acinar cells also increased with time. Shown are currents recorded at $+60$ and -120 mV (outward and inward currents respectively) at 3 (thin line)

and 15 min (thick line) after achieving whole cell mode with the patch electrode. While the overall kinetics of CIC-2 channels expressed in HEK 293 cells were substantially faster than the inward rectifying Cl^- current in rat parotid acinar cells, CIC-2 current also increased with time with an apparent increase in kinetics as the data in the right panel of Fig. 9 show.

Discussion

The results of this study showed that CIC-2 channels expressed in HEK 293 cells had many properties in common with voltage-activated, inward rectifying Cl^- currents present in rat parotid acinar cells. These similarities included: (i) a similar voltage dependence of channel activation and (ii) the respective currents slowly increased in magnitude with time during the experiment and this was associated with an increase in gating kinetics. We found that CIC-2 transcripts were present in individual acinar cells and that the parotid gland contained CIC-2 protein. Taken together these results suggest that it is quite likely that the inward rectifying Cl^- current in rat parotid acinar cells involves the protein encoded by the CIC-2 gene.

However, there are very large differences in kinetics between the currents in acinar cells and the CIC-2 currents expressed in HEK 293 cells. One explanation for the difference is simply the cell background in which the channels are expressed. The kinetics of CIC-2 channels expressed in *Xenopus* oocytes (Thiemann et al., 1992; Jordt & Jentsch, 1997) are more than two orders of magnitude slower than when expressed in HEK 293 cells. According to this view, the channel in acinar cells is entirely composed of the CIC-2 protein but behaves differently in parotid cells than it does in heterologous expression systems.

One mechanism for this difference could be differences in phosphorylation state of the CIC-2 protein which contains numerous consensus phosphorylation sequences for protein kinases A and C. Protein kinase A increases the open probability of CIC-2 channels expressed in *Xenopus* oocytes and assayed with the lipid bilayer reconstitution system (Malinowska et al., 1995) and Protein kinase C reduces CIC-2 channel current expressed in neuronal cells (Staley et al., 1996). Similar actions of these kinases have also been observed on endogenous CIC-2-like currents (Madison, Malenka & Nicoll, 1986; Noulin & Joffre, 1993; Fritsch & Edelman, 1996). Thus, the time dependent appearance of voltage-activated current (Fig. 9 and see Chesnoy-Marchais & Fritsch, 1994; Fritsch & Edelman, 1996) could be due to changes in the phosphorylation state of CIC-2 induced by dialysis with an artificial internal solution.

It is also possible that the inward rectifier current of parotid acinar cells is through a heteromultimeric mem-

brane protein composed of CIC-2 and other subunits that alter channel gating kinetics. Homomultimeric structure appears to be a general property of the CIC gene family (Steinmeyer et al., 1994; Ludewig, Pusch & Jentsch, 1996; Middleton, Phessant & Miller, 1996), however it is not known if these channels associate with as yet unidentified regulatory subunits.

The pMT3-GFP vector was a gift from Dr. P. Stampe, Department of Pharmacology and Physiology, University of Rochester. We thank Dr. A.J. Persechini for a critical appraisal of this manuscript. This work was supported in part by National Institutes of Health grant R01 DE09692 (J.E.M.). Current address for J.A. is Instituto de Fisica, Universidad Autonoma de San Luis Potosi, San Luis Potosi, Mexico.

References

- Arreola, J., Park, K., Melvin, J.E., Begenisich, T. 1996. Three distinct chloride channels control anion movements in rat parotid acinar cells. *J. Physiol.* **490**:351–362
- Carew, M.A., Thorn, P. 1996. Identification of CIC-2-like chloride currents in pig pancreatic acinar cells. *Pfluegers Arch.* **433**:84–90
- Chalfie, M., Tu, Y., Euskirchen, G., Ward, W.W., Prasher, D.C. 1994. Green fluorescent protein as a marker for gene expression. *Science* **263**:801–805
- Chen, C., Okayama, H. 1987. High-efficiency transformation of mammalian cells by plasmid DNA. *Mol. Cell. Biol.* **7**:2745–2752
- Chesnoy-Marchais, D., Fritsch, J. 1994. Activation of hyperpolarization and atypical osmosensitivity of a Cl^- current in rat osteoblastic cells. *J. Membrane Biol.* **140**:173–188
- Dinudom, A., Young, J.A., Cook, D.I. 1993. Na^+ and Cl^- conductances are controlled by cytosolic Cl^- concentration in the intralobular duct cells of mouse mandibular glands. *J. Membrane Biol.* **135**:289–295
- Franke, R.R., Sakmar, T.P., Oprian, D.D., Gobind Khorana, H. 1988. A single amino acid substitution in rhodopsin (lysine 248 leucine) prevents activation of transducin. *J. Biol. Chem.* **263**:2119–2122
- Fritsch, J., Edelman, A. 1996. Modulation of the hyperpolarization-activated Cl^- current in human intestinal T_{84} epithelial cells by phosphorylation. *J. Physiol.* **490**:115–128
- Gründer, S., Thiemann, A., Pusch, M., Jentsch, T.J. 1992. Regions involved in the opening of CIC-2 chloride channel by voltage and cell volume. *Nature* **360**:759–762
- Hirt, B. 1967. Selective extraction of polyoma DNA from infected mouse cell cultures. *J. Mol. Biol.* **26**:365–369
- Jentsch, T.J. 1996. Chloride channels: a molecular perspective. *Curr. Opin. Neurobiol.* **6**:303–310
- Jentsch, T.J., Günther, W. 1997. Chloride channels: an emerging molecular picture. *BioEssays* **19**:117–126
- Jentsch, T.J., Günther, W., Pusch, M., Schwappach, B. 1995. Properties of voltage-gated chloride channels of the CIC gene family. *J. Physiol.* **482**:19S–25S
- Jordt, S.-E., Jentsch, T.J. 1997. Molecular dissection of gating in the CIC-2 chloride channel. *EMBO J.* **16**:1582–1592
- Komwatana, P., Dinudom, A., Young, J.A., Cook, D.I. 1994. Characterization of the Cl^- conductance in the granular duct cells of mouse mandibular glands. *Pfluegers Arch.* **428**:641–647
- Komwatana, P., Dinudom, A., Young, J.A., Cook, D.I. 1995. Osmotic sensitivity of the hyperpolarization-activated Cl^- current in mouse mandibular duct cells. *Cell Physiol. Biochem.* **5**:243–251
- Kowdley, G.C., Ackerman, S.J., John, J.E. III, Jones, L.R., Moorman, J.R. 1994. Hyperpolarization-activated chloride currents in *Xenopus* oocytes. *J. Gen. Physiol.* **103**:217–230
- Ludewig, U., Pusch, M., Jentsch, T.J. 1966. Two physically distinct pores in the dimeric CIC-0 chloride channel. *Nature* **383**:340–343
- Madison, D.V., Malenka, R.C., Nicoll, R.A. 1986. Phorbol esters block a voltage-sensitive chloride current in hippocampal pyramidal cells. *Nature* **321**:695–697
- Malinowska, D.H., Kupert, E.Y., Bahinski, A., Sherry, A.M., Cupoletti, J. 1995. Cloning, Functional expression, and characterization of a PKA-activated gastric Cl^- channel. *Am. J. Physiol.* **268**:C191–C200
- Marshall, J., Molloy, R., Moss, G.W., Howe, J.R., Hughes, T.E. 1995. The jellyfish green fluorescent protein: A new tool for studying ion channel expression and function. *Neuron* **14**:211–215
- Middleton, R.E., Phessant, D.J., Miller, C. 1996. Homodimeric architecture of a CIC-type Cl^- channel. *Nature* **383**:337–340
- Noulin, J.F., Joffre, M. 1993. Characterization and cyclic AMP-dependence of a hyperpolarization-activated chloride conductance in Leydig cells from mature rat testis. *J. Membrane Biol.* **133**:1–15
- Prasher, D.C., Eckenrode, V.K., Ward, W.W., Prendergast, F.G., and Cormier, M.J. 1992. Primary structure of the *Aequorea victoria* green-fluorescent protein. *Gene* **111**:229–233
- Saiki, R.K., Gelfand, D.H., Stoffel, S., Scharf, S.J., Higuchi, R., Horn, G.T., Mullis, K.B., Erlich, H.A. 1988. Primer-directed enzymatic amplification of DNA with a thermostable DNA polymerase. *Science* **239**:487–491
- Sanger, F., Nicklen, S., Coulson, A.R. 1977. DNA sequencing with chain-terminating inhibitors. *Proc. Natl. Acad. Sci. USA* **74**:5463–5467
- Smith, R.L., Clayton, G.H., Wilcox, C.L., Escudero, K.W., Staley, K.J. 1995. Differential expression of an inwardly rectifying chloride conductance in rat brain neurons: a potential mechanism for cell-specific modulation of postsynaptic inhibition. *J. Neurosci.* **15**:4057–4067
- Staley, K., Smith, R., Schaack, J., Wilcox, C., Jentsch, T.J. 1996. Alteration of GABA_A receptor function following gene transfer of the CIC-2 chloride channel. *Neuron* **17**:543–551
- Steinmeyer, K., Lorenz, C., Pusch, M., Koch, M.C., Jentsch, T.J. 1994. Multimeric structure of CIC-1 chloride channels as revealed by mutations in dominant myotonia congenita (Thomsen). *EMBO J.* **13**:7373–743
- Thiemann, A., Gründer, S., Pusch, M., Jentsch, T.J. 1992. A chloride channel widely expressed in epithelial and non-epithelial cells. *Nature* **356**:57–60
- Turner, R.J., George, J., Baum, B.J. 1986. Evidence for a $\text{Na}^+/\text{K}^+/\text{Cl}^-$ cotransport system in basolateral membrane vesicles from rabbit parotid. *J. Membrane Biol.* **94**:143–152